ISBN: 978-3-95450-215-8 ISSN: 2226-0366 doi:10.18429/JACoW-LINAC2022-MOPORI10

FIRST STUDIES OF 5D PHASE-SPACE TOMOGRAPHY OF ELECTRON BEAMS AT ARES

S. Jaster-Merz*[1], R. W. Assmann[2], R. Brinkmann, F. Burkart, T. Vinatier
Deutsches Elektronen-Synchrotron DESY, Germany
[1]also at Department of Physics Universität Hamburg, Germany
[2]also at Laboratori Nazionali di Frascati, Italy

Abstract

A new beam diagnostics method to reconstruct the full 5-dimensional phase space (x, x', y, y', t) of bunches has recently been proposed. This method combines a quadrupole-based transverse phase-space tomography with the variable streaking angle of a polarizable X-band transverse deflecting structure (PolariX TDS). Two of these novel structures have recently been installed at the ARES beamline at DESY, which is a linear accelerator dedicated to accelerator research and development, including advanced diagnostics methods and novel accelerating techniques. In this paper, realistic simulation studies in preparation for planned experimental measurements are presented using the beamline setup at ARES. The reconstruction quality of the method for three beam distributions is studied and discussed, and it is shown how this method will allow the visualization of detailed features in the phase-space distribution.

INTRODUCTION

The ARES linear accelerator [1–4] at DESY is designed to deliver stable and well-characterized electron bunches at a repetition rate up to 50 Hz with energies up to 155 MeV and charges from 0.05 pC to 200 pC. Its research program focuses on performing advanced accelerator research and development. This includes the production and measurement of bunches with down to sub-fs durations [5–9] for the study of novel dielectric-based acceleration techniques [10–13] and medical applications; the application of machine learning to accelerator operation [14, 15]; and the development of diagnostic devices and methods [16–21]. As part of these activities, a tomographic method is being developed that would allow for the reconstruction of the 5-dimensional (5D) phase space of electron bunches. The method takes advantage of the polarizable X-band transverse deflecting structure (PolariX TDS) that has recently been developed in a collaboration between CERN, DESY, and PSI [22–24]. Two of these structures are installed at ARES and will be operational in 2023. The variable streaking angle has already enabled the reconstruction of the 3D charge density (x, y, t) at other beamlines [8, 9, 23, 25]. In the technique presented here, it is used to perform a slice-wise 4D transverse phase-space tomography [26–29], effectively reconstructing the 5D (x, x', y, y', t) phase space of the bunches. This information is useful to optimize and improve the beam quality, detect correlations and other features in the distribution, or perform detailed simulation studies. The method and its working principle were first presented in [21]. Here, simulation studies in preparation for experimental measurements using the beamline setup at ARES are presented. These studies investigate the accuracy of the method for three different beam distributions.

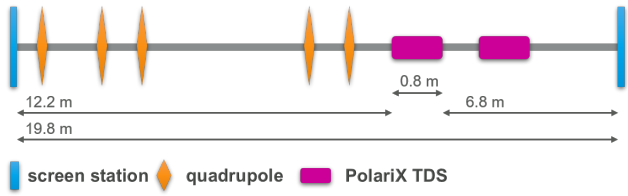

Figure 1: Sketch of the ARES beamline layout used for the 5D phase-space tomography simulation studies.

WORKING PRINCIPLE

The method is based on performing a longitudinally sliced transverse phase-space tomography. In order to perform a transverse tomography, the transverse phase space needs to be rotated. This rotation is performed in normalized phase space, where the phase advance $\mu_{x,y}$ is equivalent to the rotation angles $\theta_{x,y}$ [30]. The conversions from real phase-space coordinates x, y and x', y' to normalized phase-space coordinates x_N, y_N and x'_N, y'_N are given by $x_N, y_N = x, y/\sqrt{\beta_{x,y}}$ and $x'_N, y'_N = x, y(\alpha_{x,y}/\sqrt{\beta_{x,y}}) + x', y'\sqrt{\beta_{x,y}}$, where $\beta_{x,y}$ and $\alpha_{x,y}$ are the Courant-Snyder parameters [31]. The longitudinal information of the bunch is obtained by streaking the bunch with the PolariX TDS at various transverse angles. By using a tomographic reconstruction algorithm such as the SART (Simultaneous Algebraic Reconstruction Technique) [32], this allows the reconstruction of the 3D charge density (x, y, t) [8, 9, 23, 25] for each (θ_x, θ_y) combination. Then, with the same algorithm, the 4D distribution (x, x', y, t) is reconstructed by using all the 3D reconstructions for a fixed θ_y. Finally, by combining the 4D reconstructions of all scanned θ_y, the 5D distribution (x, x', y, y', t) is obtained.

ACCURACY OF 5D PHASE-SPACE TOMOGRAPHY

The accuracy of the tomographic reconstructions is affected by several factors. Firstly, a larger number of transverse rotations and streaking angles is in general beneficial, especially when the distribution has detailed features. Secondly, chromatic effects due to a finite energy spread result

* sonja.jaster-merz@desy.de

ISBN: 978-3-95450-215-8 ISSN: 2226-0366 doi:10.18429/JACoW-LINAC2022-MOPORI10

Table 1: Beam Parameters of the Original and Reconstructed Distributions

		Distribution 1		Distribution 2		Distribution 3	
Parameter	**Unit**	Original	Recon.	Original	Recon.	Original	Recon.
E	MeV	155	-	155	-	155	-
σ_E	%	0.1	-	0.1	-	0.1	-
Q	pC	1	-	1	-	1	-
σ_τ	fs	200.02	200.97	200.00	200.96	199.99	202.80
ϵ_x	m rad	3.30×10^{-9}	3.29×10^{-9}	3.30×10^{-9}	3.37×10^{-9}	7.25×10^{-9}	11.62×10^{-9}
ϵ_y	m rad	3.32×10^{-9}	3.36×10^{-9}	3.31×10^{-9}	3.48×10^{-9}	6.24×10^{-9}	11.00×10^{-9}
ϵ_x^n	µm	1.00	1.00	1.00	1.02	2.20	3.52
ϵ_y^n	µm	1.01	1.02	1.01	1.06	1.89	3.34
α_x		0.00	0.00	0.00	0.00	0.00	0.00
α_y		0.00	0.00	0.00	0.00	0.00	0.00
β_x	m	5.00	4.99	5.00	4.89	5.01	4.92
β_y	m	5.00	4.95	5.00	4.84	5.01	5.04

in a spread of the phase advance within the distribution. This leads to variations in the transverse rotation angles, impacting the quality of the transverse reconstruction, as well as in the final spot size at the screen, impacting the longitudinal resolution. This is of particular relevance, because the TDS itself can be a source of energy spread due to the transverse variation of the longitudinal field as a result of the Panofsky-Wenzel theorem [33]. Finally, the resolution of the screen needs to be fine enough to resolve all features of the distribution.

In the present study, the capabilities of the method to reconstruct phase-space densities with correlations and complex features are investigated. This is done by studying three different distributions. Distribution 1 is a purely Gaussian distribution without correlations. Distribution 2 is a Gaussian distribution with imprinted correlations in the $(x'–z)$, $(y'–z)$ and $(x'–y')$ planes. Distribution 3 consists of three superimposed Gaussian beams with transverse offsets with respect to each other and longitudinal correlations in the transverse momenta, resulting in a complex phase-space structure. All distributions feature the same initial Courant-Snyder parameters, which allows for the use of the same quadrupole settings for the three distributions. Distributions 1 and 2 have the same transverse emittance while distribution 3 features a larger transverse emittance due to its multi-bunch structure. All the initial beam parameters are listed in Table 1, where E is the energy, σ_E the energy spread, Q the charge, σ_t the RMS bunch duration, and $\epsilon_{x,y}$ ($\epsilon^n_{x,y}$) the geometric (normalized) RMS emittance.

5D reconstructions of all three distributions are performed using the beamline shown in Fig. 1, aiming for a longitudinal resolution of 20 fs for distribution 1 and 2 (40 fs for distribution 3 due to its larger RMS spot sizes at the screen). The longitudinal resolution R is defined as $R = \sigma pc/(2\pi feVL)$ [34], where σ is the maximum unstreaked transverse spot size at the screen downstream of the TDS, p is the average momentum of the bunch, c the speed of light, e the elementary charge, f the TDS frequency, V the peak voltage, and L the drift length between the TDS center and the downstream screen. Given the desired resolution, a TDS frequency of 11.99 GHz, σ = 244 µm, and L = 7.21 m a peak voltage of 3.6 MV is required. Since each of the available PolariX TDSs will be able to streak the beam with up to 20 MV peak voltage, only the first TDS in Fig. 1 is used in this study.

The streaking angle of this TDS is varied over a range of 180° in 50 steps. Five quadrupoles are used to scan the transverse phase advances over a range of 180° in 40 steps. The projections of the distributions are recorded on the screen station downstream of the TDS. The simulated screen has a size of 2.02 x 2.02 cm to fit ±4 sigma of the RMS bunch duration, and 1000 x 1000 pixels, which corresponds to a resolution in the range of the ARES screen stations. The reconstruction of the transverse distribution is performed at the location of the screen station upstream of the first displayed quadrupole.

All simulations are performed in OCELOT [35, 36] using distributions with 4 000 000 particles. Second-order transfer maps are used for all elements except the TDS, where only a first-order transfer map is available.

The final reconstruction has a size of 200 bins in all transverse dimensions and 40 bins in the longitudinal plane, which, respectively, results in a resolution of 5 µm/$\sqrt{\text{m}}$ and 40 fs.

All tomographic reconstructions are performed using a python scikit-image [37] implementation of the SART algorithm [32]. Two iterations over this algorithm are performed for each tomographic reconstruction. A condition is imposed in the algorithm to ensure charge preservation and strictly positive charge-density values.

RESULTS

The reconstructed Courant-Snyder parameters, emittances, and bunch lengths are listed in Table 1. When only a limited number of rotation angles are used, tomographic methods such as the SART tend to introduce spurious charge density even far off-axis where no charge should be present

ISBN: 978-3-95450-215-8 ISSN: 2226-0366 doi:10.18429/JACoW-LINAC2022-MOPORI10

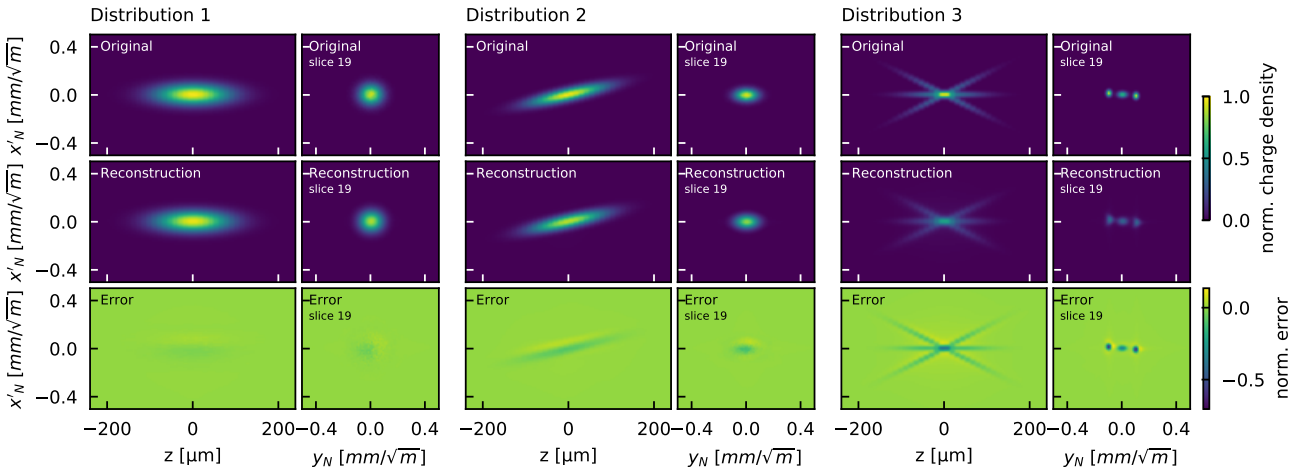

Figure 2: Original (top) and reconstructed (middle) phase space for all distributions. For each distribution, the left plot shows the $(x'–z)$ phase space, the right plot the $(x'–y)$ phase space for the central longitudinal slice ranging from −6.0 µm to 6.0 µm. The bottom row shows the difference between the reconstructed and original distribution. All distributions are normalized to the maximum value of the corresponding original distribution.

[23]. Therefore, to analyze the emittances and Courant-Snyder parameters of the reconstructed distributions only values within a ±3 sigma range from the bunch center are considered. Excellent agreement with relative discrepancies of $\lesssim 5\,\%$ is achieved for the beam parameters of distributions 1 and 2. The imprinted correlations in distribution 2 are analyzed in normalized phase space. For the original distribution, the slopes of the $(x'–y')$, $(x'–z)$ and $(y'–z)$ correlations are, respectively, −1.18, 1.20 $\mathrm{m}^{-1/2}$, and −1.42 $\mathrm{m}^{-1/2}$. The values obtained from the tomographic reconstructions are −1.25 for $(x'–y')$, 1.27 $\mathrm{m}^{-1/2}$ for $(x'–z)$, and −1.48 $\mathrm{m}^{-1/2}$ for $(y'–z)$ showing a relative discrepancy below 6 %. For distribution 3, the reconstructed bunch duration and Courant-Snyder parameters agree well with the original parameters with discrepancies below 2 %. However, the reconstructed emittances show large deviations. Possible reasons could be an insufficient number of projection angles and screen resolution to resolve the sharp features of the distribution.

Exemplarily, in Fig. 2 the reconstructed $(x'–z)$ phase space and the central longitudinal slice of the $(x'–y)$ phase space are plotted (second row) for all three distributions and compared to the original distribution (top row). The charge densities are normalized to the corresponding maximum value of the original distribution. The bottom row shows the difference between the reconstructed and original phase spaces. Excellent agreement between the reconstructed and original distribution can be seen for distribution 1 (left) and distribution 2 (center). For distribution 3, the correct reconstruction of the distribution features can be appreciated. Despite the slight washing out of the features all sub-structures of the bunch are visible.

CONCLUSION

The presented simulation studies show that the 5D phase-space tomography method allows for the reconstruction and visualization of the full transverse phase-space distribution of all longitudinal slices of the bunch. For a Gaussian distribution and a distribution with a longitudinally correlated transverse momentum offset, excellent agreement with the original beam parameters (discrepancies $\lesssim 5\,\%$) and correlations (discrepancies $\lesssim 6\,\%$) is obtained. More noticeable discrepancies appear when reconstructing a complex, multi-beam distribution, although all relevant features are clearly recovered. Potential sources for these discrepancies, which will be studied in more detail in future work, include the number of projection angles, the screen resolution, chromaticity in the quadrupoles, and an induced energy spread by the TDS.

ACKNOWLEDGMENTS

We would like to thank B. Marchetti for the suggestion of studying the 5D phase-space tomography with the PolariX TDS. We would also like to thank A. Ferran Pousa for many helpful discussions on beam dynamics and the efficient computational implementation of the method, D. Marx and P. Gonzalez Caminal for helpful discussions on beam dynamics in the PolariX TDS, and W. Kuropka for providing the implementation of the ARES beamline in OCELOT. Finally, we thank A. Wolski for helpful discussions on the 4D tomography method and inspiring discussions on the 5D simulation studies. This research was supported in part through the Maxwell computational resources operated at Deutsches Elektronen-Synchrotron DESY, Hamburg, Germany. We acknowledge support from DESY (Hamburg, Germany), a member of the Helmholtz Association HGF.

REFERENCES

[1] B. Marchetti *et al.*, "SINBAD-ARES - a photo-injector for external injection experiments in novel accelerators at DESY,"

ISBN: 978-3-95450-215-8 ISSN: 2226-0366 doi:10.18429/JACoW-LINAC2022-MOPORI10

J. Phys. Conf. Ser., vol. 1596, no. 1, p. 012 036, 2020. doi:10.1088/1742-6596/1596/1/012036

[2] E. Panofski *et al.*, "Commissioning results and electron beam characterization with the S-band photoinjector at SINBAD-ARES," *Instruments*, vol. 5, no. 3, 2021. doi:10.3390/instruments5030028

[3] U. Dorda *et al.*, "Status and objectives of the dedicated accelerator R&D facility "SINBAD" at DESY," *Nucl. Instrum. Methods Phys. Res., Sect. A*, vol. 909, pp. 239–242, 2018, 3rd European Advanced Accelerator Concepts workshop (EAAC2017). doi:10.1016/j.nima.2018.01.036

[4] F. Burkart *et al.*, "ARES Linac at DESY in Operation," presented at LINAC'22, Liverpool, United Kingdom, August 2022, paper THPOJO01.

[5] B. Marchetti *et al.*, "Electron-beam manipulation techniques in the SINBAD linac for external injection in plasma wakefield acceleration," *Nucl. Instrum. Methods Phys. Res., Sect. A*, vol. 829, pp. 278–283, 2016, 2nd European Advanced Accelerator Concepts Workshop - EAAC 2015. doi:10.1016/j.nima.2016.03.041

[6] J. Zhu, "Design Study for Generating Sub-femtosecond to Femtosecond Electron Bunches for Advanced Accelerator Development at SINBAD," Dissertation, University of Hamburg, 2017, Dissertation, University of Hamburg, 2017, p. 171. doi:10.3204/PUBDB-2018-01379

[7] J. Zhu, R. W. Assmann, M. Dohlus, U. Dorda, and B. Marchetti, "Sub-fs electron bunch generation with sub-10-fs bunch arrival-time jitter via bunch slicing in a magnetic chicane," *Phys. Rev. Accel. Beams*, vol. 19, p. 054 401, 2016. doi:10.1103/PhysRevAccelBeams.19.054401

[8] D. Marx, R. W. Assmann, P. Craievich, K. Floettmann, A. Grudiev, and B. Marchetti, "Simulation studies for characterizing ultrashort bunches using novel polarizable X-band transverse deflection structures," *Sci. Rep.*, vol. 9, no. 1, p. 19 912, 2019. doi:10.1038/s41598-019-56433-8

[9] D. Marx, "Characterization of Ultrashort Electron Bunches at the SINBAD-ARES Linac," Dissertation, Universität Hamburg, 2019, Dissertation, Universität Hamburg, 2019, p. 176. doi:10.3204/PUBDB-2019-04190

[10] F. Mayet, "Acceleration and Phase Space Manipulation of Relativistic Electron Beams in Nano- and Micrometer-Scale Dielectric Structures," Ph.D. thesis, Universität Hamburg, 2019. doi:10.3204/PUBDB-2019-03861

[11] W. Kuropka, "Studies towards Acceleration of Relativistic Electron Beams in Laser-driven Dielectric Microstructures," Ph.D. thesis, Universität Hamburg, 2020. doi:10.3204/PUBDB-2020-02257

[12] F. Mayet *et al.*, "Simulations and plans for possible DLA experiments at SINBAD," *Nucl. Instrum. Methods Phys. Res., Sect. A*, vol. 909, pp. 213–216, 2018. doi:10.1016/j.nima.2018.01.088

[13] W. Kuropka, F. Mayet, R. Aßmann, and U. Dorda, "Full PIC simulation of a first ACHIP experiment @ SINBAD," *Nucl. Instrum. Methods Phys. Res., Sect. A*, vol. 909, pp. 193–195, 2018. doi:10.1016/j.nima.2018.02.042

[14] A. Eichler *et al.*, "First Steps Toward an Autonomous Accelerator, a Common Project Between DESY and KIT," in *Proc. IPAC'21*, Campinas, Brazil, May 2021, pp. 2182–2185. doi:10.18429/JACoW-IPAC2021-TUPAB298

[15] J. Kaiser, O. Stein, and A. Eichler, "Learning-based optimisation of particle accelerators under partial observability without real-world training," in *Proceedings of the 39th International Conference on Machine Learning*, 2022.

[16] S. Jaster-Merz *et al.*, "Development of a silicon strip detector for novel accelerators at SINBAD," *J. Phys. Conf. Ser.*, vol. 1350, no. 1, p. 012 148, 2019. doi:10.1088/1742-6596/1350/1/012148

[17] S. Jaster-Merz *et al.*, "Development of a beam profile monitor based on silicon strip sensors for low-charge electron beams," *J. Phys. Conf. Ser.*, vol. 1596, no. 1, p. 012 047, 2020. doi:10.1088/1742-6596/1596/1/012047

[18] F. Mayet, R. Assmann, and F. Lemery, "Longitudinal phase space synthesis with tailored 3D-printable dielectric-lined waveguides," *Phys. Rev. Accel. Beams*, vol. 23, p. 121 302, 2020. doi:10.1103/PhysRevAccelBeams.23.121302

[19] W. Kuropka, R. Aßmann, U. Dorda, and F. Mayet, "Simulation of deflecting structures for dielectric laser driven accelerators," *Nucl. Instrum. Methods Phys. Res., Sect. A*, vol. 909, pp. 196–198, 2018. doi:10.1016/j.nima.2018.02.032

[20] F. Mayet *et al.*, "Predicting the transverse emittance of space charge dominated beams using the phase advance scan technique and a fully connected neural network," Phys. Rev. Accel. Beams, to be published.

[21] S. Jaster-Merz, R. W. Aßmann, R. Brinkmann, F. Burkart, and T. Vinatier, "5D Tomography of Electron Bunches at ARES," in *Proc. IPAC'22*, Bangkok, Thailand, 2022, pp. 279–283. doi:10.18429/JACoW-IPAC2022-MOPOPT021

[22] P. Craievich *et al.*, "Novel *X*-band transverse deflection structure with variable polarization," *Phys. Rev. Accel. Beams*, vol. 23, p. 112 001, 2020. doi:10.1103/PhysRevAccelBeams.23.112001

[23] B. Marchetti *et al.*, "Experimental demonstration of novel beam characterization using a polarizable X-band transverse deflection structure," *Sci. Rep.*, vol. 11, no. 1, p. 3560, 2021. doi:10.1038/s41598-021-82687-2

[24] A. Grudiev, "design of compact high power rf components at x-band," 2016. https://cds.cern.ch/record/2158484

[25] D. Marx, R. Assmann, P. Craievich, U. Dorda, A. Grudiev, and B. Marchetti, "Reconstruction of the 3D charge distribution of an electron bunch using a novel variable-polarization transverse deflecting structure (TDS)," *J. Phys. Conf. Ser.*, vol. 874, p. 012 077, 2017. doi:10.1088/1742-6596/874/1/012077

[26] K. Hock and A. Wolski, "Tomographic reconstruction of the full 4D transverse phase space," *Nucl. Instrum. Methods Phys. Res., Sect. A*, vol. 726, pp. 8–16, 2013. doi:10.1016/j.nima.2013.05.004

[27] A. Wolski, D. C. Christie, B. L. Militsyn, D. J. Scott, and H. Kockelbergh, "Transverse phase space characterization in an accelerator test facility," *Phys. Rev. Accel. Beams*, vol. 23, p. 032 804, 2020. doi:10.1103/PhysRevAccelBeams.23.032804

ISBN: 978-3-95450-215-8 ISSN: 2226-0366 doi:10.18429/JACoW-LINAC2022-MOPORI10

[28] V. Guo, P. E. Denham, P. Musumeci, A. Ody, and Y. Park, "4D Beam Tomography at the UCLA Pegasus Laboratory," Pohang, Korea, Sep. 2021, presented at IBIC'21, Pohang, Korea, Sep. 2021, paper TUPP15, unpublished. https://jacow.org/ibic2021/papers/TUPP15.pdf

[29] S. Jaster-Merz *et al.*, "Characterization of the Full Transverse Phase Space of Electron Bunches at ARES," in *Proc. IPAC'21*, Campinas, Brazil, May 2021, pp. 952–955. doi:10.18429/JACoW-IPAC2021-MOPAB302

[30] K. Hock, M. Ibison, D. Holder, A. Wolski, and B. Muratori, "Beam tomography in transverse normalised phase space," *Nucl. Instrum. Methods Phys. Res., Sect. A*, vol. 642, no. 1, pp. 36–44, 2011. doi:10.1016/j.nima.2011.04.002

[31] E. Courant and H. Snyder, "Theory of the alternating-gradient synchrotron," *Ann. Phys.*, vol. 3, no. 1, pp. 1–48, 1958. doi:10.1016/0003-4916(58)90012-5

[32] A. Andersen and A. Kak, "Simultaneous Algebraic Reconstruction Technique (SART): A superior implementation of the ART algorithm," *Ultrason. Imaging*, vol. 6, no. 1, pp. 81–94, 1984. doi:10.1016/0161-7346(84)90008-7

[33] W. Panofsky and W. Wenzel, "Some considerations concerning the transverse deflection of charged particles in radio-frequency fields," *Rev. Sci. Instrum.*, vol. 27, no. 11, pp. 967–967, 1956.

[34] D. Marx, R. Assmann, U. Dorda, B. Marchetti, and F. Mayet, "Lattice considerations for the use of an X-band transverse deflecting structure (TDS) at SINBAD, DESY," *J. Phys. Conf. Ser.*, vol. 874, p. 012 078, 2017. doi:10.1088/1742-6596/874/1/012078

[35] I. Agapov, G. Geloni, S. Tomin, and I. Zagorodnov, "OCELOT: A software framework for synchrotron light source and FEL studies," *Nucl. Instrum. Methods Phys. Res., Sect. A*, vol. 768, pp. 151–156, 2014. doi:10.1016/j.nima.2014.09.057

[36] S. I. Tomin, I. V. Agapov, M. Dohlus, and I. Zagorodnov, "OCELOT as a Framework for Beam Dynamics Simulations of X-Ray Sources," in *Proc. IPAC'17*, Copenhagen, Denmark, May 2017, pp. 2642–2645. doi:10.18429/JACoW-IPAC2017-WEPAB031

[37] S. Van der Walt *et al.*, "Scikit-image: Image processing in Python," *PeerJ*, vol. 2, p. e453, 2014. doi:10.7717/peerj.453